Follows MJ, Williams RG and Marshall JC (1996) The solubility pump of carbon in the subtropical gyre of the North Atlantic. *Journal of Marine Research* 54: 605–630.

Hansell DA and Carlson CA (1998) Net community production of dissolved organic carbon. *Global Biogeochemical Cycles* 12: 443–453.

Holmén K (1992) The global carbon cycle. In: Butcher SS, Charlson RJ, Orians GH and Wolfe GV (eds) *Global Biogeochemical Cycles*, pp. 239–262. New York: Academic Press.

Houghton JT, Meira Filho LG, Callander BA *et al.* (eds) (1996) *Climate Change 1995: The Science of Climate Change*. New York: Cambridge University Press.

Michaels AF and Silver MW (1988) Primary producers, sinking fluxes and the microbial food web. *Deep-Sea Research* 35: 473–490.

Sarmiento JL and Wofsy (eds) (1999) *A U.S. Carbon Cycle Science Plan*. Washington, DC: U.S. Global Change Research Program.

Sarmiento JL, Hughes TMC, Stouffer RJ and Manabe S (1998) Simulated response of the ocean carbon cycle to anthropogenic climate warming. *Nature* 393: 245–249.

Schlesinger WH (1997) *Biogeochemistry: An Analysis of Global Change*. New York: Academic Press.

Siegenthaler U and Sarmiento JL (1993) Atmospheric carbon dioxide and the ocean. *Nature* 365: 119–125.

Steinberg DK, Carlson CA, Bates NR, Goldthwait SA, Madin LP and Michaels AF (2000) Zooplankton vertical migration and the active transport of dissolved organic and inorganic carbon in the Sargasso Sea. *Deep-Sea Research I* 47: 137–158.

Takahashi T, Tans PP and Fung I (1992) Balancing the budget: carbon dioxide sources and sinks, and the effect of industry. *Oceanus* 35: 18–28.

Varney M (1996) The marine carbonate system. In: Summerhayes CP and Thorpe SA (eds) *Oceanography an Illustrated Guide*, pp. 182–194. London: Manson Publishing.

CARBON DIOXIDE (CO_2) CYCLE

T. Takahashi, Lamont Doherty Earth Observatory, Columbia University, Palisades, NY, USA

doi:10.1006/rwos.2001.0066

Introduction

The oceans, the terrestrial biosphere, and the atmosphere are the three major dynamic reservoirs for carbon on the earth. Through the exchange of CO_2 between them, the atmospheric concentration of CO_2 that affects the heat balance of the earth, and hence the climate, is regulated. Since carbon is one of the fundamental constituents of living matter, how it cycles through these natural reservoirs has been one of the fundamental questions in environmental sciences. The oceans contain about 50 times as much carbon (about 40 000 Pg-C or 10^{15} g as carbon) as the atmosphere (about 750 Pg-C). The terrestrial biosphere contains about three times as much carbon (610 Pg-C in living vegetation and 1580 Pg-C in soil organic matter) as the atmosphere. The air–sea exchange of CO_2 occurs via gas exchange processes across the sea surface; the natural air-to-sea and sea-to-air fluxes have been estimated to be about 90 Pg-C y^{-1} each. The unperturbed uptake flux of CO_2 by global terrestrial photosynthesis is roughly balanced with the release flux by respiration, and both have been estimated to be about 60 Pg-C y^{-1}. Accordingly, atmospheric CO_2 is cycled through the ocean and terrestrial biosphere with a timescale of about 7 years.

The lithosphere contains a huge amount of carbon (about 100 000 000 Pg-C) in the form of limestones ((Ca, Mg) CO_3), coal, petroleum, and other forms of organic matter, and exchanges carbon slowly with the other carbon reservoirs via such natural processes as chemical weathering and burial of carbonate and organic carbon. The rate of removal of atmospheric CO_2 by chemical weathering has been estimated to be of the order of 1 Pg-C y^{-1}. Since the industrial revolution in the nineteenth century, the combustion of fossil fuels and the manufacturing of cement have transferred the lithospheric carbon into the atmosphere at rates comparable to the natural CO_2 exchange fluxes between the major carbon reservoirs, and thus have perturbed the natural balance significantly (6 Pg-C y^{-1} is about an order of magnitude less than the natural exchanges with the oceans (90 Pg-C y^{-1} and land (60 Pg-C y^{-1})). The industrial carbon emission rate has been about 6 Pg-C y^{-1} for the 1990s, and the cumulative industrial emissions since the nineteenth century to the end of the twentieth century have been estimated to be about 250 Pg-C. Presently, the atmospheric CO_2 content is increasing at a rate of about 3.5 Pg-C y^{-1} (equivalent to about 50% of the annual emission) and the remainder of the CO_2 emitted into the atmosphere is absorbed by the oceans and terrestrial biosphere in approximately equal proportions. These industrial

CO_2 emissions have caused the atmospheric CO_2 concentration to increase by as much as 30% from about 280 ppm (parts per million mole fraction in dry air) in the pre-industrial year 1850 to about 362 ppm in the year 2000. The atmospheric CO_2 concentration may reach 580 ppm, double the pre-industrial value, by the mid-twentyfirst century. This represents a significant change that is wholly attributable to human activities on the Earth.

It is well known that the oceans play an important role in regulating our living environment by providing water vapor into the atmosphere and transporting heat from the tropics to high latitude areas. In addition to these physical influences, the oceans partially ameliorate the potential CO_2-induced climate changes by absorbing industrial CO_2 in the atmosphere.

Therefore, it is important to understand how the oceans take up CO_2 from the atmosphere and how they store CO_2 in circulating ocean water. Furthermore, in order to predict the future course of the atmospheric CO_2 changes, we need to understand how the capacity of the ocean carbon reservoir might be changed in response to the Earth's climate changes, that may, in turn, alter the circulation of ocean water. Since the capacity of the ocean carbon reservoir is governed by complex interactions of physical, biological, and chemical processes, it is presently not possible to identify and predict reliably various climate feedback mechanisms that affect the ocean CO_2 storage capacity.

Units

In scientific and technical literature, the amount of carbon has often been expressed in three different units: gigatons of carbon (Gt-C), petagrams of carbon (Pg-C) and moles of carbon or CO_2. Their relationships are: $1\,\text{Gt-C} = 1\ \text{Pg-C} = 1 \times 10^{15}$ g of carbon = 1000 million metric tonnes of carbon $= (1/12) \times 10^{15}$ moles of carbon. The equivalent quantity as CO_2 may be obtained by multiplying the above numbers by 3.67 (= 44/12 = the molecular weight of CO_2 divided by the atomic weight of carbon).

The magnitude of CO_2 disequilibrium between the atmosphere and ocean water is expressed by the difference between the partial pressure of CO_2 of ocean water, (pCO_2)sw, and that in the overlying air, (pCO_2)air. This difference represents the thermodynamic driving potential for CO_2 gas transfer across the sea surface. The pCO_2 in the air may be estimated using the concentration of CO_2 in air, that is commonly expressed in terms of ppm (parts per million) in mole fraction of CO_2 in dry air, in the relationship:

$$(pCO_2)\text{air} = (CO_2\ \text{conc.})\text{air} \times (Pb - pH_2O) \quad [1]$$

where Pb is the barometric pressure and pH_2O is the vapor pressure of water at the sea water temperature. The partial pressure of CO_2 in sea water, (pCO_2)sw, may be measured by equilibration methods or computed using thermodynamic relationships. The unit of microatmospheres (μatm) or 10^{-6} atm is commonly used in the oceanographic literature.

History

The air–sea exchange of CO_2 was first investigated in the 1910s through the 1930s by a group of scientists including K. Buch, H. Wattenberg, and G.E.R. Deacon. Buch and his collaborators determined in land-based laboratories CO_2 solubility, the dissociation constants for carbonic and boric acids in sea water, and their dependence on temperature and chlorinity (the chloride ion concentration in sea water). Based upon these dissociation constants along with the shipboard measurements of pH and titration alkalinity, they computed the partial pressure of CO_2 in surface ocean waters. The Atlantic Ocean was investigated from the Arctic to Antarctic regions during the period 1917–1935, especially during the METEOR Expedition 1925–27, in the North and South Atlantic. They discovered that temperate and cold oceans had lower pCO_2 than air (hence the sea water was a sink for atmospheric CO_2), especially during spring and summer seasons, due to the assimilation of CO_2 by plants. They also observed that the upwelling areas of deep water (such as African coastal areas) had greater pCO_2 than the air (hence the sea water was a CO_2 source) due to the presence of respired CO_2 in deep waters.

With the advent of the high-precision infrared CO_2 gas analyzer, a new method for shipboard measurements of pCO_2 in sea water and in air was introduced during the International Geophysical Year, 1956–59. The precision of measurements was improved by more than an order of magnitude. The global oceans were investigated by this new method, which rapidly yielded high precision data. The equatorial Pacific was identified as a major CO_2 source area. The GEOSECS Program of the International Decade of Ocean Exploration, 1970–80, produced a global data set that began to show systematic patterns for the distribution of CO_2 sink and source areas over the global oceans.

Methods

The net flux of CO_2 across the sea surface, Fs-a, may be estimated by:

$$\text{Fs-a} = \boldsymbol{E} \times [(pCO_2)\text{sw} - (pCO_2)\text{air}]$$
$$= \boldsymbol{k} \times \alpha \times [(pCO_2)\text{sw} - (pCO_2)\text{air}] \quad [2]$$

where $\boldsymbol{E}$ is the CO_2 gas transfer coefficient expressed commonly in (moles $CO_2/m^2/y/$uatm); $\boldsymbol{k}$ is the gas transfer piston velocity (e.g. in (cm h^{-1})) and α is the solubility of CO_2 in sea water at a given temperature and salinity (e.g. (moles CO_2 kg-sw^{-1} atm^{-1})). If (pCO_2) sw > (pCO_2) air, the net flux of CO_2 is from the sea to the air and the ocean is a source of CO_2; if (pCO_2)sw < (pCO_2) air, the ocean water is a sink for atmospheric CO_2. The sea–air pCO_2 difference may be measured at sea and α has been determined experimentally as a function of temperature and salinity. However, the values of $\boldsymbol{E}$ and $\boldsymbol{k}$ that depend on the magnitude of turbulence near the air–water interface cannot be simply characterized over complex ocean surface conditions. Nevertheless, these two variables have been commonly parameterized in terms of wind speed over the ocean. A number of experiments have been performed to determine the wind speed dependence under various wind tunnel conditions as well as ocean and lake environments using different nonreactive tracer gases such as SF_6 and ^{222}Rn. However, the published results differ by as much as 50% over the wind speed range of oceanographic interests.

Since ^{14}C is in the form of CO_2 in the atmosphere and enters into the surface ocean water as CO_2 in a timescale of decades, its partition between the atmosphere and the oceans yields a reliable estimate for the mean CO_2 gas transfer rate over the global oceans. This yields a CO_2 gas exchange rate of 20 ± 3 mol CO_2 m^{-2} y^{-1} that corresponds to a sea–air CO_2 transfer coefficient of 0.067 mol CO_2 m^{-2} y^{-1} uatm^{-1}. Wanninkhof in 1992 presented an expression that satisfies the mean global CO_2 transfer coefficient based on ^{14}C and takes other field and wind tunnel results into consideration. His equation for variable wind speed conditions is:

$$\boldsymbol{k}\ (\text{cm h}^{-1}) = 0.39 \times (u_{av})^2 \times (Sc/660)^{-0.5} \quad [3]$$

where u_{av} is the average wind speed in m s^{-1} corrected to 10 m above sea surface; Sc (dimensionless) is the Schmidt number (kinematic viscosity of water)/(diffusion coefficient of CO_2 gas in water); and 660 represents the Schmidt number for CO_2 in sea water at 20°C (*see also* **Air–Sea Gas Exchange**).

In view of the difficulties in determining gas transfer coefficients accurately, direct methods for CO_2 flux measurements aboard the ship are desirable. Sea–air CO_2 flux was measured directly by means of the shipboard eddy-covariance method over the North Atlantic Ocean by Wanninkhof and McGillis in 1999. The net flux of CO_2 across the sea surface was determined by a covariance analysis of the triaxial motion of air with CO_2 concentrations in the moving air measured in short time intervals ($\sim$ ms) as a ship moved over the ocean. The results obtained over a wind speed range of 2–13.5 m s^{-1} are consistent with eqn [3] within about $\pm$ 20%. If the data obtained in wind speeds up to 15 m s^{-1} are taken into consideration, they indicate that the gas transfer piston velocity tends to increase as a cube of wind speed. However, because of a large scatter ($\pm$ 35%) of the flux values at high wind speeds, further work is needed to confirm the cubic dependence.

In addition to the uncertainties in the gas transfer coefficient (or piston velocity), the CO_2 flux estimated with eqn [2] is subject to errors in (pCO_2)sw caused by the difference between the bulk water temperature and the temperature of the thin skin of ocean water at the sea–air interface. Ordinarily the (pCO_2)sw is obtained at the bulk seawater temperature, whereas the relevant value for the flux calculation is (pCO_2)sw at the 'skin' temperature, that depends on the rate of evaporation, the incoming solar radiation, the wind speed, and the degree of turbulence near the interface. The 'skin' temperature is often cooler than the bulk water temperature by as much as 0.5°C if the water evaporates rapidly to a dry air mass, but is not always so if a warm humid air mass covers over the ocean. Presently, the time–space distribution of the 'skin' temperature is not well known. This, therefore, could introduce errors in (pCO_2)sw up to about 6 μatm or 2%.

CO_2 Sink/Source Areas of the Global Ocean

The oceanic sink and source areas for atmospheric CO_2 and the magnitude of the sea–air CO_2 flux over the global ocean vary seasonally and annually as well as geographically. These changes are the manifestation of changes in the partial pressure of sea water, (pCO_2)sw, which are caused primarily by changes in the water temperature, in the biological utilization of CO_2, and in the lateral/vertical circulation of ocean waters including the upwelling of deep water rich in CO_2. Over the global oceans, seawater temperatures change from the pole to the equator by about 32°C. Since the pCO_2 in sea water

doubles with each 16°C of warming, temperature changes should cause a factor of 4 change in pCO_2. Biological utilization of CO_2 over the global oceans is about 200 μmol CO_2 kg^{-1}, which should reduce pCO_2 in sea water by a factor of 3. If this is accompanied with growths of $CaCO_3$-secreting organisms, the reduction of pCO_2 could be somewhat smaller. While these effects are similar in magnitude, they tend to counteract each other seasonally, since the biological utilization tends to be large when waters are warm. In subpolar and polar areas, winter cooling of surface waters induces deep convective mixing that brings high pCO_2 deep waters to the surface. The lowering effect on CO_2 by winter cooling is often compensated for or sometimes overcompensated for by the increasing effect of the upwelling of high CO_2 deep waters. Thus, in high latitude oceans, surface waters may become a source for atmospheric CO_2 during the wintertime when the water is coldest.

In **Figure 1**, the global distribution map of the sea–air pCO_2 differences for February and August 1995, are shown. These maps were constructed on the basis of about a half million pairs of atmospheric and seawater pCO_2 measurements made at sea over the 40-year period, 1958–98, by many investigators. Since the measurements were made in different years, during which the atmospheric pCO_2 was increasing, they were corrected to a single reference year (arbitrarily chosen to be 1995) on the basis of the following observations. Warm surface waters in subtropical gyres communicate slowly with the underlying subsurface waters due to the presence of a strong stratification at the base of the mixed layer. This allows a long time for the surface mixed-layer waters ($\sim$ 75 m thick) to exchange CO_2 with the atmosphere. Therefore, their CO_2 chemistry tends to follow the atmospheric CO_2 increase. Accordingly, the pCO_2 in the warm water follows the increasing trend of atmospheric CO_2, and the sea–air pCO_2 difference tends to be independent of the year of measurements. On the other hand, since surface waters in high latitude regions are replaced partially with subsurface waters by deep convection during the winter, the effect of increased atmospheric CO_2 is diluted to undetectable levels and their CO_2 properties tend to remain unchanged from year to year. Accordingly, the sea–air pCO_2 difference measured in a given year increases as the atmospheric CO_2 concentration increases with time. This effect was corrected to the reference year using the observed increase in the atmospheric CO_2 concentration. During El Niño periods, sea–air pCO_2 differences over the equatorial belt of the Pacific Ocean, which are large in normal years, are reduced significantly and observations are scarce. Therefore, observations made between 10°N and 10°S in the equatorial Pacific for these periods were excluded from the maps. Accordingly, these maps represent the climatological means for non-El Niño period oceans for the past 40 years. The purple-blue areas indicate that the ocean is a sink for atmospheric CO_2, and the red-yellow areas indicate that the ocean is a source.

Strong CO_2 sinks (blue and purple areas) are present during the winter months in the Northern (**Figure 1A**) and Southern (**Figure 1B**) Hemispheres along the poleward edges of the subtropical gyres, where major warm currents are located. The Gulf Stream in the North Atlantic and the Kuroshio Current in the North Pacific are both major CO_2 sinks (**Figure 1A**) due primarily to cooling as they flow from warm tropical oceans to subpolar zones.

Similarly, in the Southern Hemisphere, CO_2 sink areas are formed by the cooling of poleward-flowing currents such as the Brazil Current located along eastern South America, the Agulhus Current located south of South Africa, and the East Australian Current located along south-eastern Australia. These warm water currents meet with cold currents flowing equatorward from the Antarctic zone along the northern border of the Southern (or Antarctic) Ocean. As the subAntarctic waters rich in nutrients flow northward to more sunlit regions, CO_2 is drawn down by photosynthesis, thus creating strong CO_2 sink conditions, as exemplified by the Falkland Current in the western South Atlantic (**Figure 1A**). Confluence of subtropical waters with polar waters forms broad and strong CO_2 sink zones as a result of the juxtaposition of the lowering effects on pCO_2 of the cooling of warm waters and the photosynthetic drawdown of CO_2 in nutrient-rich subpolar waters. This feature is clearly depicted in a zone between 40°S and 60°S in **Figure 1A** representing the austral summer, and between 20°S and 40°S in **Figure 1B** representing the austral winter.

During the summer months, the high latitude areas of the North Atlantic Ocean (**Figure 1A**) and the Weddell and Ross Seas, Antarctica (**Figure 1B**), are intense sink areas for CO_2. This is attributed to the intense biological utilization of CO_2 within the strongly stratified surface layer caused by solar warming and ice melting during the summer. The winter convective mixing of deep waters rich in CO_2 and nutrients eliminates the strong CO_2 sink and replenishes the depleted nutrients in the surface waters.

The Pacific equatorial belt is a strong CO_2 source which is caused by the warming of upwelled deep waters along the coast of South America as well as

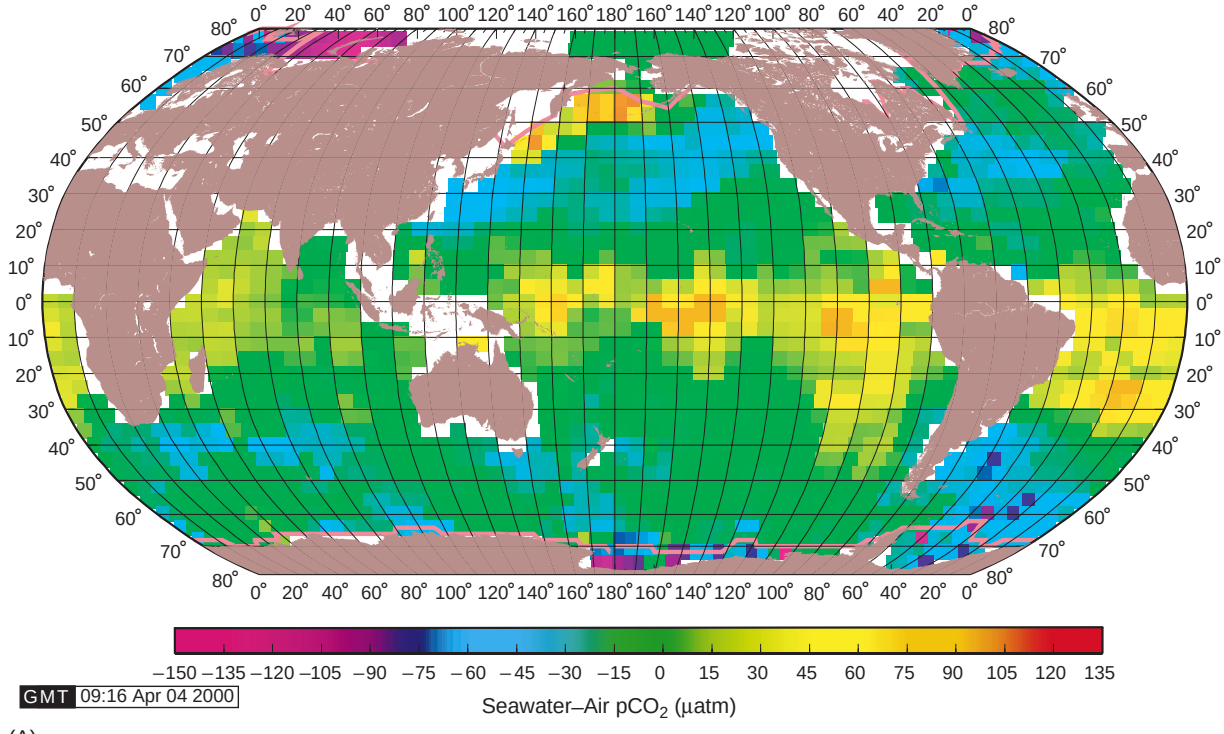

(A)

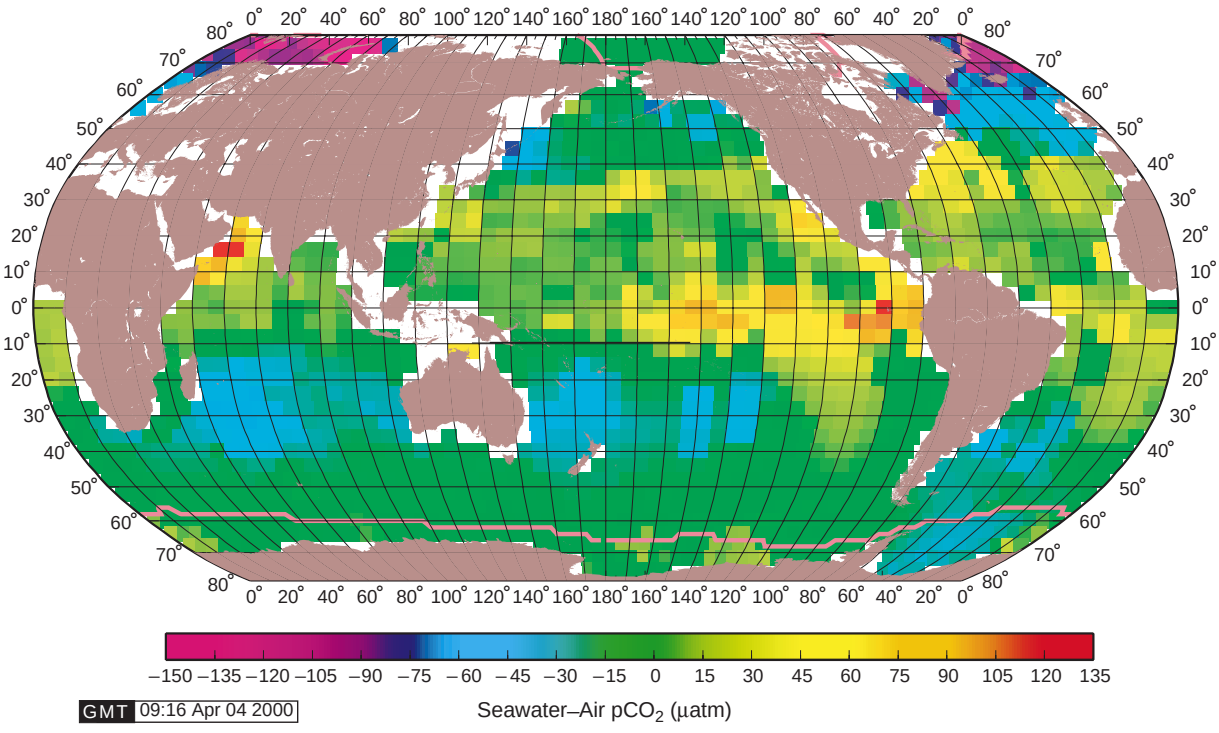

(B)

Figure 1 The sea–air pCO_2 difference in μatm (ΔpCO_2) for (A) February and (B) August for the reference year 1995. The purple-blue areas indicate that the ocean is a sink for atmospheric CO_2, and the red-yellow areas indicate that the ocean is source. The pink lines in the polar regions indicate the edges of ice fields.

by the upward entrainment of the equatorial undercurrent water. The source strengths are most intense in the eastern equatorial Pacific due to the strong upwelling, and decrease to the west as a result of the biological utilization of CO_2 and nutrients during the westward flow of the surface water.

Small but strong source areas in the north-western subArctic Pacific Ocean are due to the winter convective mixing of deep waters (**Figure 1A**). The lowering effect on pCO_2 of cooling in the winter is surpassed by the increasing effect of high CO_2 concentration in the upwelled deep waters. During the summer (**Figure 1B**), however, these source areas become a sink for atmospheric CO_2 due to the intense biological utilization that overwhelms the increasing effect on pCO_2 of warming. A similar area is found in the Arabian Sea, where upwelling of deep waters is induced by the south-west monsoon during July–August (**Figure 1B**), causing the area to become a strong CO_2 source. This source area is eliminated by the photosynthetic utilization of CO_2 following the end of the upwelling period (**Figure 1A**).

As illustrated in **Figure 1A** and **B**, the distribution of oceanic sink and source areas for atmospheric CO_2 varies over a wide range in space and time. Surface ocean waters are out of equilibrium with respect to atmospheric CO_2 by as much as $\pm 200\,\mu atm$ (or by $\pm 60\%$). The large magnitudes of CO_2 disequilibrium between the sea and the air is in contrast with the behavior of oxygen, another biologically mediated gas, that shows only up to $\pm 10\%$ sea–air disequilibrium. The large CO_2 disequilibrium may be attributed to the fact that the internal ocean processes that control pCO_2 in sea water, such as the temperature of water, the photosynthesis, and the upwelling of deep waters, occur at much faster rates than the sea–air CO_2 transfer rates. The slow rate of CO_2 transfer across the sea surface is due to the slow hydration rates of CO_2 as well as to the large solubility of CO_2 in sea water attributable to the formation of bicarbonate and carbonate ions. The latter effect does not exist at all for oxygen.

Net CO_2 Flux Across the Sea Surface

The net sea–air CO_2 flux over the global oceans may be computed using eqns [2] and [3]. **Figure 2** shows the climatological mean distribution of the annual sea–air CO_2 flux for the reference year 1995 using the following set of information. (1) The

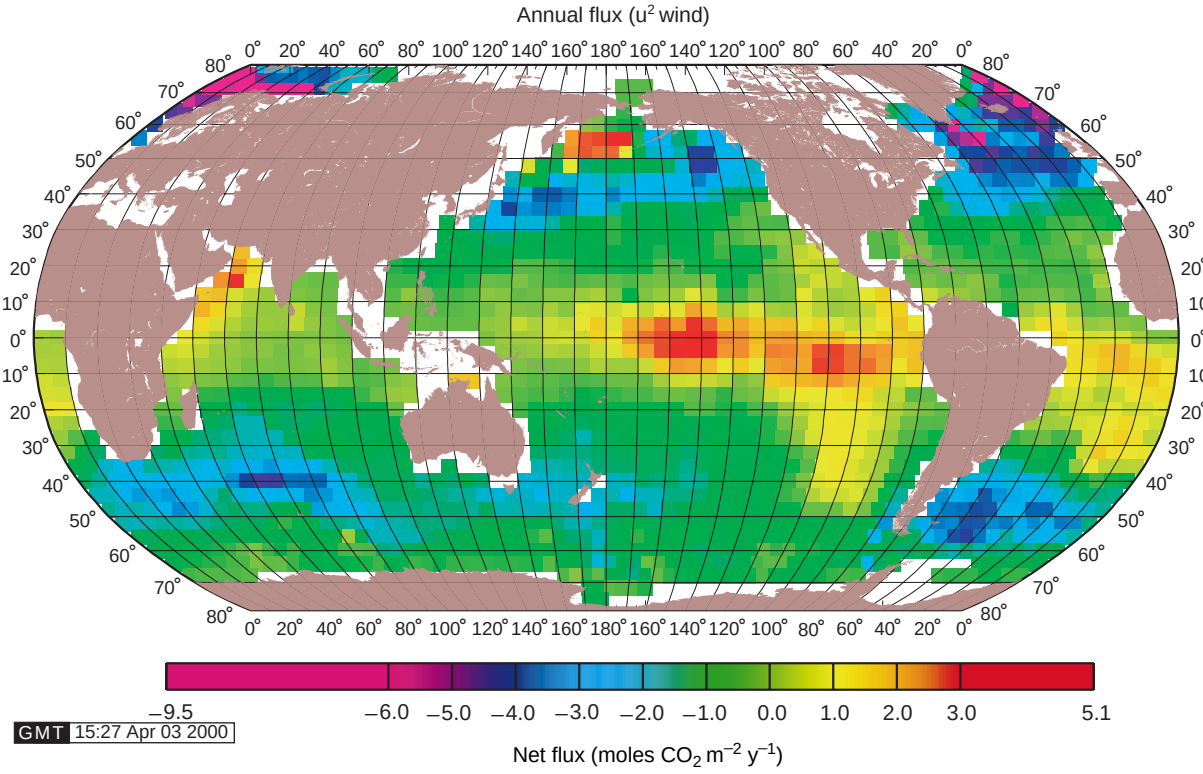

Figure 2 The mean annual sea–air flux of CO_2 in the reference year 1995. The red-yellow areas indicate that the flux is from sea to air, whereas blue-purple areas indicate that the flux is from air to sea. The flux is given in moles of $CO_2\,m^{-2}y^{-1}$. The map gives a total annual air-to-sea flux of 2.0 Pg-C y^{-1}.

monthly mean ΔpCO_2 values in $4^\circ \times 5^\circ$ pixel areas for the reference year 1995 (**Figure 1A** and **B** and for all other months); (2) the Wanninkhof formulation, eqn [3], for the effect of wind speed on the CO_2 gas transfer coefficient; and (3) the climatological mean wind speeds for each month compiled by Esbensen and Kushnir in 1981. This set yields a mean global gas transfer rate of 0.063 mole $CO_2\,m^{-2}\,\mu atm^{-1}\,y^{-1}$, that is consistent with 20 moles $CO_2\,m^{-2}\,y^{-1}$ estimated on the basis of carbon-14 distribution in the atmosphere and the oceans.

Figure 2 shows that the equatorial Pacific is a strong CO_2 source. On the other hand, the areas along the poleward edges of the temperate gyres in both hemispheres are strong sinks for atmospheric CO_2. This feature is particularly prominent in the southern Indian and Atlantic Oceans between 40°S and 60°S, and is attributable to the combined effects of negative sea–air pCO_2 differences with strong winds ('the roaring 40s') that accelerate sea–air gas transfer rates. Similarly strong sink zones are formed in the North Pacific and North Atlantic between 45°N and 60°N. In the high latitude Atlantic, strong sink areas extend into the Norwegian and Greenland Seas. Over the high latitude Southern Ocean areas, the sea–air gas transfer is impeded by the field of ice that covers the sea surface for ≥ 6 months in a year.

The net sea–air CO_2 fluxes computed for each ocean basin for the reference year of 1995, representing non-El Niño conditions, are summarized in **Table 1**. The annual net CO_2 uptake by the global ocean is estimated to be about 2.0 Pg-C y^{-1}. This is consistent with estimates obtained on the basis of a number of different ocean–atmosphere models including multi-box diffusion advection models and three-dimensional general circulation models.

The uptake flux for the Northern Hemisphere ocean (north of 14°N) is 1.2 Pg-C y^{-1}, whereas that for the Southern Hemisphere ocean (south of 14°S) is 1.7 Pg-C y^{-1}. Thus, the Southern Hemisphere ocean is a stronger CO_2 sink by about 0.5 Pg C y^{-1}. This is due partially to the much greater oceanic areas in the Southern Hemisphere. In addition, the Southern Ocean south of 50°S is an efficient CO_2 sink, for it takes up about 26% of the global ocean CO_2 uptake, while it has only 10% of the global ocean area. Cold temperature and moderate photosynthesis are both responsible for the large uptake by the Southern Ocean.

The Atlantic Ocean is the largest net sink for atmospheric CO_2 (39%); the Southern Ocean (26%) and the Indian Ocean (24%) are next; and the Pacific Ocean (11%) is the smallest. The intense biological drawdown of CO_2 in the high latitude areas of the North Atlantic and Arctic seas during the summer months is responsible for the Atlantic being a major sink. This is also due to the fact that the upwelling deep waters in the North Atlantic contain low CO_2 concentrations, which are in turn caused primarily by the short residence time ($\sim$ 80y) of the North Atlantic Deep Waters. The small uptake flux of the Pacific can be attributed to the fact that the combined sink flux of the northern and southern subtropical gyres is roughly balanced by the source flux from the equatorial Pacific during non-El Niño periods. On the other hand, the equatorial Pacific CO_2 source flux is significantly reduced or eliminated during El Niño events. As a result the equatorial zone is covered with the eastward spreading of the warm, low pCO_2 western Pacific waters in response to the relaxation of the trade wind.

Table 1 The net sea–air flux of CO_2 estimated for a reference year of 1995 using the effect of wind speed on the CO_2 gas transfer coefficient, eqn [3], of Wanninkhof and the monthly wind field of Esbensen and Kushnir

Latitudes	*Pacific Ocean*	*Atlantic Ocean*	*Indian Ocean*	*Southern Ocean*	*Global Oceans*
	Sea–air flux in 10^{15} g Carbon y^{-1}				
North of 50°N	− 0.02	− 0.44	—	—	− 0.47
50°N–14°N	− 0.47	− 0.27	+ 0.03	—	− 0.73
14°N–14°S	+ 0.64	+ 0.13	+ 0.09	—	+ 0.86
14°S–50°S	− 0.37	− 0.20	− 0.60	—	− 1.17
South of 50°S	—	—	—	− 0.52	− 0.52
Total	− 0.23	− 0.78	− 0.47	− 0.52	− 2.00
% Uptake	11%	39%	24%	26%	100%
Area (10^6 km^2)	151.6	72.7	53.2	31.7	309.1
Area (%)	49.0%	23.5%	17.2%	10.2%	100%

Positive values indicate sea-to-air fluxes, and negative values indicate air-to-sea fluxes.

Although the effects of El Niño and Southern Ocean Oscillation may be far reaching beyond the equatorial zone as far as to the polar areas, the El Niño effects on the equatorial Pacific alone could reduce the equatorial CO_2 source. Hence, this could increase the global ocean uptake flux by up to 0.6 Pg-C y^{-1} during an El Niño year.

The sea–air CO_2 flux estimated above is subject to three sources of error: (1) biases in sea–air ΔpCO_2 values interpolated from relatively sparse observations, (2) the 'skin' temperature effect, and (3) uncertainties in the gas transfer coefficient estimated on the basis of the wind speed dependence. Possible biases in ΔpCO_2 differences have been tested using sea surface temperatures (SST) as a proxy. The systematic error in the global sea–air CO_2 flux resulting from sampling and interpolation has been estimated to be about $\pm 30\%$ or ± 0.6 Pg-C y^{-1}. The 'skin' temperature of ocean water may affect ΔpCO_2 by as much as $\pm 6\,\mu$atm depending upon time and place, as discussed earlier.

Although the distribution of the 'skin' temperature over the global ocean is not known, it may be cooler than the bulk water temperature by a few tenths of a degree on the global average. This may result in an underestimation of the ocean uptake by 0.4 Pg-C y^{-1}. The estimated global sea–air flux depends on the wind speed data used. Since the gas transfer rate increases nonlinearly with wind speed, the estimated CO_2 fluxes tend to be smaller when mean monthly wind speeds are used instead of high frequency wind data.

Furthermore, the wind speed dependence on the CO_2 gas transfer coefficient in high wind speed regimes is still questionable. If the gas transfer rate is taken to be a cubic function of wind speed instead of the square dependence as shown above, the global ocean uptake would be increased by about 1 Pg-C y^{-1}. The effect is particularly significant over the high latitude oceans where the winds are strong. Considering various uncertainties discussed above, the global ocean CO_2 uptake presented in **Table 1** is uncertain by about 1 Pg-C y^{-1}.

See also

Air–Sea Gas Exchange. Carbon Cycle. Ocean Carbon System, Modelling of. Ocean Circulation. Primary Production Distribution. Radiocarbon. Stable Carbon Isotope Variations in the Ocean. Thermohaline Circulation. Wind Driven Circulation.

Further Reading

Broecker WS and Peng TH (1982) *Tracers in the Sea*. Palisades, NY: Eldigio Press.

Broecker WS, Ledwell JR, Takahashi *et al.* (1986) Isotopic versus micrometeorologic ocean CO_2 fluxes: a serious conflict. *Journal of Geophysical Research* 91: 10517–10527.

Keeling R, Piper SC and Heinmann M (1996) Global and hemispheric CO_2 sinks deduced from changes in atmospheric O_2 concentration. *Nature* 381: 218–221.

Sarmiento JL, Murnane R and Le Quere C (1995) Air–sea CO_2 transfer and the carbon budget of the North Atlantic. *Philosophical Transactions of the Royal Society of London, series B* 343: 211–219.

Sundquist ET (1985) Geological perspectives on carbon dioxide and carbon cycle. In: Sundquist ET and Broecker WS (eds) *The Carbon Cycle and Atmospheric CO_2: Natural Variations, Archean to Present, Geophysical Monograph 32*, pp. 5–59. Washington, DC: American Geophysical Union.

Takashahi T, Olafsson J, Goddard J, Chipman DW and Sutherland SC (1993) Seasonal variation of CO_2 and nutrients in the high-latitude surface oceans: a comparative study. *Global Biogeochemical Cycles* 7: 843–878.

Takahashi T, Feely RA, Weiss R *et al.* (1997) Global air–sea flux of CO_2: an estimate based on measurements of sea–air pCO_2 difference. *Proceedings of the National Academy of Science USA* 94: 8292–8299.

Tans PP, Fung IY and Takahashi T (1990) Observational constraints on the global atmospheric CO_2 budget. *Sciece* 247: 1431–1438.

Wanninkhof R (1992) Relationship between wind speed and gas exchange. *Journal of Geophysical Research* 97: 7373–7382.

Wanninkhof R and McGillis WM (1999) A cubic relationship between gas transfer and wind speed *Geophysical Research Letters* 26: 1889–1893.

CARBON ISOTOPES

See **STABLE CARBON ISOTOPE VARIATIONS IN THE OCEAN**